

Unitarity Tests of the Neutrino Mixing Matrix

X. Qian,^{1,*} C. Zhang,¹ M. Diwan,¹ and P. Vogel²

¹*Physics Department, Brookhaven National Laboratory, Upton, NY*

²*Kellogg Radiation Laboratory, California Institute of Technology, Pasadena, CA*

(Dated: February 26, 2022)

We discuss unitarity tests of the neutrino mixing (PMNS) matrix. We show that the combination of solar neutrino experiments, medium-baseline and short-baseline reactor antineutrino experiments make it possible to perform the first direct unitarity test of the PMNS matrix. In particular, the measurements of Daya Bay and JUNO (a next generation medium-baseline reactor experiment) will lay the foundation of a precise unitarity test of $|U_{e1}|^2 + |U_{e2}|^2 + |U_{e3}|^2 = 1$. Furthermore, the precision measurement of $\sin^2 2\theta_{13}$ in both the $\bar{\nu}_e$ disappearance and the ν_e appearance (from a ν_μ beam) channels will provide an indirect unitarity test of the PMNS matrix. Together with the search for appearance/disappearance at very short distances, these tests could provide important information about the possible new physics beyond the three-neutrino model.

Introduction: In the past decades our understanding of neutrinos has advanced dramatically. Initially, neutrinos were thought to be massless, since only left-handed neutrinos and right-handed antineutrinos were detected in experiments [1]. The existence of non-zero neutrino masses and the neutrino mixing were then successfully established through the observation of neutrino flavor oscillations. Recent reviews can be found e.g. in Ref. [2, 3]. In the three-neutrino framework, the oscillations are characterized by the neutrino mixing (commonly referred to as the Pontecorvo-Maki-Nakagawa-Sakata or PMNS in short) matrix [4–6] and two neutrino mass-squared differences ($\Delta m_{32}^2 = m_3^2 - m_2^2$ and $\Delta m_{21}^2 = m_2^2 - m_1^2$).

The PMNS matrix U_{PMNS} (or U in short),

$$\begin{pmatrix} \nu_e \\ \nu_\mu \\ \nu_\tau \end{pmatrix} = \begin{pmatrix} U_{e1} & U_{e2} & U_{e3} \\ U_{\mu 1} & U_{\mu 2} & U_{\mu 3} \\ U_{\tau 1} & U_{\tau 2} & U_{\tau 3} \end{pmatrix} \cdot \begin{pmatrix} \nu_1 \\ \nu_2 \\ \nu_3 \end{pmatrix}, \quad (1)$$

describes the mixing between the neutrino flavor (ν_e, ν_μ, ν_τ) and mass eigenstates (ν_1, ν_2 , and ν_3 with masses m_1, m_2 , and m_3 , respectively). Components of the PMNS matrix can be determined through measurements of neutrino oscillations. For neutrinos with energy E and flavor l , the probability of its transformation to flavor l' after traveling a distance L in vacuum is expressed as:

$$P(\nu_l \rightarrow \nu_{l'}) = \left| \sum_i U_{li} U_{l'i}^* e^{-i(m_i^2/2E)L} \right|^2 \\ = \sum_i |U_{li} U_{l'i}^*|^2 + \Re \sum_i \sum_{j \neq i} U_{li} U_{l'i}^* U_{lj}^* U_{l'j} e^{i \frac{\Delta m_{ij}^2 L}{2E}}. \quad (2)$$

The unitarity tests of the PMNS matrix refer to establishing whether $U \times U^* \stackrel{?}{=} I$ and $U^* \times U \stackrel{?}{=} I$, where I is the 3×3 unit matrix. These conditions are represented

by twelve equations in total:

$$|U_{l1}|^2 + |U_{l2}|^2 + |U_{l3}|^2 \stackrel{?}{=} 1|_{l=e,\mu,\tau} \quad (3)$$

$$U_{l1} U_{l'1}^* + U_{l2} U_{l'2}^* + U_{l3} U_{l'3}^* \stackrel{?}{=} 0|_{l,l'=e,\mu,\tau;l \neq l'} \quad (4)$$

$$|U_{ei}|^2 + |U_{\mu i}|^2 + |U_{\tau i}|^2 \stackrel{?}{=} 1|_{i=1,2,3} \quad (5)$$

$$U_{ei} U_{ej}^* + U_{\mu i} U_{\mu j}^* + U_{\tau i} U_{\tau j}^* \stackrel{?}{=} 0|_{i,j=1,2,3;i \neq j}. \quad (6)$$

The PMNS matrix is conventionally written as explicitly unitary:

$$\begin{pmatrix} c_{12}c_{13} & s_{12}c_{13} & s_{13}e^{-i\delta} \\ -s_{12}c_{23} - c_{12}s_{23}s_{13}e^{i\delta} & c_{12}c_{23} - s_{12}s_{23}s_{13}e^{i\delta} & s_{23}c_{13} \\ s_{12}s_{23} - c_{12}c_{23}s_{13}e^{i\delta} & -c_{12}s_{23} - s_{12}c_{23}s_{13}e^{i\delta} & c_{23}c_{13} \end{pmatrix},$$

with three mixing angles $\theta_{12}, \theta_{23}, \theta_{13}$ ($s_{ij} = \sin \theta_{ij}$ and $c_{ij} = \cos \theta_{ij}$), and a phase δ , commonly referred to as the CP phase in the leptonic sector.

Super-Kamiokande [7], K2K [8], MINOS [9], T2K [10], and IceCube [11] experiments determined the angle θ_{23} and the mass difference $|\Delta m_{32}^2|$ using the ν_μ disappearance channel with atmospheric and accelerator neutrinos. The KamLAND [12] and SNO [13] experiments measured θ_{12} and Δm_{21}^2 with $\bar{\nu}_e$ disappearance channel using reactor antineutrinos and ν_e disappearance channel using solar neutrinos¹, respectively. Recently, the Daya Bay [14, 15], Double Chooz [16], and RENO [17] measured θ_{13} and are on their ways to measure $|\Delta m_{31}^2|$ with $\bar{\nu}_e$ disappearance using reactor antineutrinos. The current knowledge of the mixing angles and mass squared

¹ Due to the MSW effect, the ν_e disappearance probability in SNO is different from Eq. (2).

differences [2] are ²:

$$\begin{aligned}
\sin^2 2\theta_{12} &= 0.857 \pm 0.024 \\
\sin^2 2\theta_{23} &> 0.95 \\
\sin^2 2\theta_{13} &= 0.095 \pm 0.010 \\
\Delta m_{21}^2 &= (7.5 \pm 0.2) \times 10^{-5} eV^2 \\
|\Delta m_{32}^2| &= (2.32^{+0.12}_{-0.08}) \times 10^{-3} eV^2.
\end{aligned} \tag{7}$$

Besides the disappearance channels listed above, the appearance channel is becoming a powerful tool to determine the matrix elements of U_{PMNS} . The MINOS [18] and T2K [19, 20] measured the ν_μ to ν_e appearance probability with accelerator neutrinos. In particular, T2K [20] established the ν_e appearance at a 7.5σ level. OPERA [21] and Super-Kamiokande [22] experiments observed the ν_μ to ν_τ appearance with accelerator and atmospheric neutrinos, respectively. In the neutrino sector the determination of the remaining unknown quantities, including the value of CP phase δ and the sign of $|\Delta m_{32}^2|$ (neutrino mass hierarchy), are the goals of the current (Nova [23] and T2K), and next generation neutrino oscillation experiments (LBNE [24, 25], JUNO [26, 27], Hyper-K [28], and PINGU [29]). With future precise measurements of neutrino oscillation characteristics, unitarity tests of the PMNS matrix become possible. In the following, we will discuss the direct and indirect unitarity tests of the PMNS matrix.

Direct unitarity test of the first row: In a direct unitarity test, individual components of the PMNS matrix are measured. Eqs. (3)-(6) may then be tested directly. The most promising one is the test of the first row $|U_{e1}|^2 + |U_{e2}|^2 + |U_{e3}|^2 \stackrel{?}{=} 1$, to be discussed in detail below.

SNO measurement of ν_e disappearance with solar neutrinos provides the first constraint. The higher energy 8B solar neutrinos detected in SNO can be well approximated as the mass eigenstates due to the MSW effect [30–33]. Therefore, by comparing the charged current (ν_e only) and the neutral current (sum of all ν_l) events, a direct constraint on $\cos^4 \theta_{13} \sin^2 \theta_{12} + \sin^4 \theta_{13}$ or in terms of the PMNS matrix elements on the combination $|U_{e2}|^2 \cdot (|U_{e1}|^2 + |U_{e2}|^2) + |U_{e3}|^4$ is provided.

In addition, $|U_{e1}|^2$, $|U_{e2}|^2$, and $|U_{e3}|^2$ can be constrained using the $\bar{\nu}_e$ disappearance with reactor experiments. In particular, $4|U_{e1}|^2 \cdot |U_{e2}|^2$ was first determined by the KamLAND experiment, and will be significantly improved by the next generation medium-baseline reactor antineutrino experiments (e.g., the upcoming "Jianmen Underground Neutrino Observatory" (JUNO)

experiment, and the RENO-50 experiment). Meanwhile, the currently running Daya Bay experiment (together with RENO and Double Chooz) will provide the most precise measurement of the $\bar{\nu}_e$ disappearance for the oscillations governed by Δm_{3x}^2 (Δm_{31}^2 and Δm_{32}^2), constraining $4|U_{e3}|^2 \cdot (|U_{e1}|^2 + |U_{e2}|^2)$. However, due to the tiny difference between Δm_{31}^2 and Δm_{32}^2 , the Daya Bay experiment can not determine $4|U_{e3}|^2 \cdot |U_{e1}|^2$ and $4|U_{e3}|^2 \cdot |U_{e2}|^2$ separately. With three independent constraints, three unknown $|U_{e1}|^2$, $|U_{e2}|^2$, and $|U_{e3}|^2$ can be completely determined. Therefore, the combination of medium-baseline reactor experiments (KamLAND, JUNO and RENO-50), short-baseline reactor experiments (Daya Bay, RENO, and Double Chooz), and SNO solar neutrino results make possible the first direct unitarity test of the PMNS matrix.

In the following, as an example, we study the expected sensitivity of testing $|U_{e1}|^2 + |U_{e2}|^2 + |U_{e3}|^2 \stackrel{?}{=} 1$ with SNO, Daya Bay, and JUNO. We adapted the fitter developed in Ref. [26], which is used to study the physics capability of JUNO. The expected results from Daya Bay and the results of SNO are taken from Ref. [34] and Ref. [13], respectively. For JUNO, a 20 kt fiducial volume liquid scintillator detector is assumed at a distance of 55 km from the reactor complex with a total thermal power of 40 GW and five years running time.

The experimental uncertainties in the absolute normalization in both the detection efficiency and the neutrino flux have to be taken into account for Daya Bay and JUNO. In particular, the debate regarding the "reactor anomaly" [35, 36] shows that the uncertainty in reactor flux can be as large as 6-8%. In Daya Bay, the uncertainty in reactor flux is mitigated by using the ratio method [37] with near and far detectors. In JUNO, the constraint of $4|U_{e1}|^2 \cdot |U_{e2}|^2$ is mainly coming from the spectrum distortion [26] due to the Δm_{21}^2 oscillation. In both cases, the oscillation formula need to be modified and becomes actually

$$\begin{aligned}
P &= (|U_{e1}|^2 + |U_{e2}|^2 + |U_{e3}|^2)^2 \\
&\cdot \left(1 - \frac{4|U_{e1}|^2|U_{e2}|^2}{(|U_{e1}|^2 + |U_{e2}|^2 + |U_{e3}|^2)^2} \sin^2 \left(\frac{\Delta m_{21}^2 L}{4E} \right) \right. \\
&\left. - \frac{4|U_{e3}|^2(|U_{e1}|^2 + |U_{e2}|^2)}{(|U_{e1}|^2 + |U_{e2}|^2 + |U_{e3}|^2)^2} \sin^2 \left(\frac{\Delta m_{3x}^2 L}{4E} \right) \right), \tag{8}
\end{aligned}$$

in which the overall $(|U_{e1}|^2 + |U_{e2}|^2 + |U_{e3}|^2)^2$ term cannot be separated from the uncertainty in the absolute normalization. Therefore, instead of constraining $4|U_{e3}|^2 \cdot (|U_{e1}|^2 + |U_{e2}|^2)$ and $4|U_{e1}|^2 \cdot |U_{e2}|^2$, the Daya Bay and JUNO experiments are in fact constraining and going to constrain $\frac{4|U_{e3}|^2 \cdot (|U_{e1}|^2 + |U_{e2}|^2)}{(|U_{e1}|^2 + |U_{e2}|^2 + |U_{e3}|^2)^2}$ and $\frac{4|U_{e1}|^2 \cdot |U_{e2}|^2}{(|U_{e1}|^2 + |U_{e2}|^2 + |U_{e3}|^2)^2}$, respectively. For example, if the 6% reactor anomaly is due to the existence of heavy sterile neutrinos, the impact of the fast oscillations of the sterile neutrino components will be absorbed into

² The uncertainties represent the 68% confidence intervals. The limit quoted for $\sin^2 2\theta_{23}$ corresponds to the projection of the 90% confidence interval in the $\sin^2 2\theta_{23}$ - Δm_{23}^2 plane onto the $\sin^2 2\theta_{23}$ axis.

$(|U_{e1}|^2 + |U_{e2}|^2 + |U_{e3}|^2)^2 \simeq 0.94$. The θ_{13} (θ_{12}) angle measured by Daya Bay (JUNO) would therefore be an effective angle: $\sin^2 2\theta_{13}^{eff} = \frac{4|U_{e3}|^2 \cdot (|U_{e1}|^2 + |U_{e2}|^2)}{0.94}$ instead of $4|U_{e3}|^2 \cdot (|U_{e1}|^2 + |U_{e2}|^2)$ ($\sin^2 2\theta_{12}^{eff} \approx \frac{4|U_{e1}|^2 |U_{e2}|^2}{0.94}$).

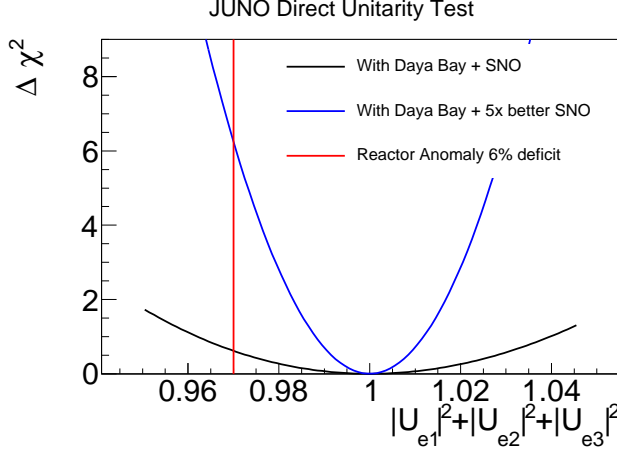


FIG. 1. Direct unitarity test of $|U_{e1}|^2 + |U_{e2}|^2 + |U_{e3}|^2 \stackrel{?}{=} 1$ by combining JUNO, Daya Bay, and solar results. We considered two scenarios i) current SNO constraint and ii) a five times better constraint than SNO. In addition, the red line shows the suggested value of $|U_{e1}|^2 + |U_{e2}|^2 + |U_{e3}|^2$ given a 6% reactor anomaly. See the text for more discussions.

In Fig. 1, the sensitivity of the direct unitarity test of the $|U_{e1}|^2 + |U_{e2}|^2 + |U_{e3}|^2 \stackrel{?}{=} 1$ by combining the expected results of JUNO, Daya Bay, and the current SNO results. It is assumed that Daya Bay will reach $\frac{4|U_{e3}|^2 \cdot (|U_{e1}|^2 + |U_{e2}|^2)}{(|U_{e1}|^2 + |U_{e2}|^2 + |U_{e3}|^2)^2} = 0.09 \pm 0.0035$ [34]. For the purpose of this study, we approximate SNO results as $|U_{e2}|^2 \cdot (|U_{e1}|^2 + |U_{e2}|^2) + |U_{e3}|^4 = 0.311 \pm 0.037$ [13]. The experimental normalization uncertainty is assumed to be 10% in JUNO, and Eq. (8) is used as the oscillation formula. The true MC spectrum is generated assuming $|U_{e1}|^2 + |U_{e2}|^2 + |U_{e3}|^2 = 1$. The hypotheses when $|U_{e1}|^2 + |U_{e2}|^2 + |U_{e3}|^2$ deviates from unity are then tested by fitting the MC data. The results are presented as $\Delta\chi^2 = \chi^2_{|U_{e1}|^2 + |U_{e2}|^2 + |U_{e3}|^2} - \chi^2_{unity}$ in Fig. 1. At 68% C.L. ($\Delta\chi^2 < 1$), the combination of JUNO, Daya Bay, and SNO results would give about 4% unitarity test. This unitarity test can be significantly improved with a stronger constraint from solar neutrino experiments. For example, with a five times improved constraint of $|U_{e2}|^2 \cdot (|U_{e1}|^2 + |U_{e2}|^2) + |U_{e3}|^4$, the unitarity test can be improved to about 1.2% level, which will be sufficiently accurate to test the reactor anomaly ³.

Other unitarity tests: The rest of equations in Eq. (3) (for the μ and τ flavor neutrinos) are more difficult to test. First, the only oscillation to be precisely measured in the foreseeable future is the ν_μ disappearance in the Δm_{3x}^2 oscillations. Second, due to the small difference between Δm_{31}^2 and Δm_{32}^2 , one would need a third independent constraint, in analogy to the solar neutrino measurements, even if the ν_μ disappearance of the Δm_{21}^2 oscillation is determined. Finally, the unitarity tests would also suffer from the uncertainties in experimental absolute normalization, which however could be improved with a future neutrino factory [38].

Direct unitarity tests of Eq. (4) can be accomplished by combining information from disappearance and appearance channels. For example, we can square both sides of $U_{e1}U_{\mu 1}^* + U_{e2}U_{\mu 2}^* + U_{e3}U_{\mu 3}^* \stackrel{?}{=} 0$:

$$0 \stackrel{?}{=} |U_{e1}|^2 |U_{\mu 1}|^2 + |U_{e2}|^2 |U_{\mu 2}|^2 + |U_{e3}|^2 |U_{\mu 3}|^2 + 2\Re(U_{e1}U_{\mu 1}^* U_{\mu 2}U_{e2}^*) + 2\Re(U_{e1}U_{\mu 1}^* U_{\mu 3}U_{e3}^*) + 2\Re(U_{e2}U_{\mu 2}^* U_{\mu 3}U_{e3}^*). \quad (9)$$

In order to directly test the above equation, one would need to measure $|U_{ei}|^2|_{i=1,2,3}$ as well as $|U_{\mu i}|^2|_{i=1,2,3}$ from disappearance channels. The latter three terms can be in principle accessed through the measurement of ν_μ to ν_e appearance probability. However, the current (Nova and T2K) and the next generation (LBNE and Hyper-K) experiments will only focus on the Δm_{3x}^2 oscillations, which leaves the Δm_{21}^2 oscillations unconstrained.

Eqs. (5) and (6) can be tested by combining measurements of ν_l disappearance and ν_l to ν_l' appearance. For example, the constant term of the summation of ν_μ disappearance, ν_μ to ν_e appearance, and ν_μ to ν_τ appearance oscillation probabilities in vacuum would be the $\sum_i (|U_{ei}|^2 + |U_{\mu i}|^2 + |U_{\tau i}|^2) \cdot |U_{\mu i}|^2$, which is related to the Eq. (5). However, this measurement would rely on an accurate determination of the experimental absolute normalization factor. Eq. (6) can be tested by searching for the absence of L/E dependence in the summation of oscillation probabilities from all three channels. However, in practice, these tests suffer from the matter effects, from the tiny difference between Δm_{32}^2 and Δm_{31}^2 , as well as from the limited precision of ν_μ to ν_τ appearance channel. Therefore, it is actually more practical to perform an indirect unitarity test through measurements of the θ_{23} or the θ_{13} mixing angles, as discussed in the following.

Indirect unitarity tests: While the direct unitarity tests appear to be extremely difficult, the violation of unitarity may be also naturally indicated in the next generation experiments searching for sterile neutrinos (e.g. Ref. [39]). A discovery of sterile neutrino could be established by unambiguously observing new oscillation patterns (different from the known Δm_{12}^2 and Δm_{3x}^2 oscillations). Most currently proposed searches are focusing on a limited range (e.g. ~ 1 eV) of the sterile neutrino

³ If this unitarity test is shown to be violated with future experimental data, beside the existence of sterile neutrino, the non-standard interaction in the sun or other new physics could also be considered as the explanation.

masses motivated by the various anomalies in the data.

On the other hand, if the sterile neutrinos or other new physics existed, the current measured mixing angles in the PMNS matrix would be effective angles, as discussed above, whose values would be process dependent. This point has been raised for example in Refs. [40, 41] before. In such kind of tests, the “proof by contradiction” principle is utilized. First, the mixing angles are extracted from the data by assuming unitarity. If the same mixing angle measured by two different processes are inconsistent, the unitarity is then shown to be violated. Otherwise, the phase space of new physics will be constrained. Here, the word “indirect” comes from the fact that components in Eqs. (3)-(6) are not measured.

There are currently three possibilities for such indirect unitarity tests: θ_{23} , θ_{12} , and θ_{13} . The θ_{23} indirect test can be achieved by comparing the ν_μ disappearance and ν_μ to ν_τ appearance. The precision will be limited by the ν_τ appearance channel. For θ_{12} , the indirect test between solar neutrino and medium-baseline reactor experiment is not necessary, as the direct test can be carried out as illustrated above.

Therefore, the most promising candidate for such indirect unitarity test is θ_{13} , which can be measured with the ν_μ to ν_e appearance (T2K, Nova, LBNE, and Hyper-K) with accelerator neutrinos, as well as the $\bar{\nu}_e$ disappearance with reactor neutrinos (Daya Bay, RENO, and Double Chooz). For example, one can test the hypothesis of the 6% reactor anomaly due to the fourth generation sterile neutrino. From Ref. [41], the $\nu_\mu \rightarrow \nu_e$ appearance probability in vacuum will be altered by the additional sterile (fourth) neutrino as:

$$\begin{aligned}
P = & 4|U_{\mu 3}|^2|U_{e 3}|^2 \sin^2 \left(\frac{\Delta m_{31}^2 L}{4E} \right) \\
& + 4|U_{\mu 2}|^2|U_{e 2}|^2 \sin^2 \left(\frac{\Delta m_{21}^2 L}{4E} \right) \\
& + 8|U_{\mu 3}||U_{e 3}||U_{\mu 2}||U_{e 2}| \\
& \times \sin \left(\frac{\Delta m_{31}^2 L}{4E} \right) \sin \left(\frac{\Delta m_{21}^2 L}{4E} \right) \cos \left(\frac{\Delta m_{32}^2 L}{4E} - \delta_3 \right) \\
& + 4|U_{\mu 3}||U_{e 3}||\beta''| \sin \left(\frac{\Delta m_{31}^2 L}{4E} \right) \sin \left(\frac{\Delta m_{31}^2 L}{4E} - \delta_1 \right) \\
& + 4|U_{\mu 2}||U_{e 2}||\beta''| \sin \left(\frac{\Delta m_{21}^2 L}{4E} \right) \sin \left(\frac{\Delta m_{21}^2 L}{4E} - \delta_2 \right) \\
& + 2|U_{\mu 4}|^2|U_{e 4}|^2, \tag{10}
\end{aligned}$$

where $\beta'' = U_{\mu 4}^* U_{e 4}$, $\delta_1 = -\arg(U_{\mu 3} U_{e 3}^* \beta'')$, $\delta_2 = -\arg(U_{\mu 2} U_{e 2}^* \beta'')$, and $\delta_3 = \arg(U_{\mu 3}^* U_{e 3} U_{\mu 2} U_{e 2}^*)$. The only approximation made here is to average terms containing large sterile mass squared differences. If we neglect the Δm_{21}^2 oscillations and assume that $\delta_1 = 0$, the change in the effective $\sin^2 2\theta_{13}$ from the long-baseline ν_e appearance experiment can be estimated as $\frac{\Delta \sin^2 2\theta_{13}}{\sin^2 2\theta_{13}} = \frac{|U_{\mu 4}||U_{e 4}|}{|U_{\mu 3}||U_{e 3}|}$. If we assume $U_{\mu 4}^* U_{e 4} = 0.04$, which satis-

fies the 90% C.L. constrained from the latest ICARUS experiment [42] ($2|U_{\mu 4}|^2|U_{e 4}|^2 < 3.4 \times 10^{-3}$), the effective $\sin^2 2\theta_{13}^{eff}$ in the appearance channel could be higher than the true one by as much as 40%. On the other hand, given the 6% reactor anomaly, the effective $\sin^2 2\theta_{13}^{eff}$ obtained through the reactor antineutrino disappearance experiments could be only about a few percent higher than the true one (e.g. $\sin^2 2\theta_{13}^{eff} = \frac{\sin^2 2\theta_{13}}{0.94}$ with $\sin^2 2\theta_{13} := 4|U_{e 3}|^2 \cdot (|U_{e 1}|^2 + |U_{e 2}|^2)$)⁴. In comparison, the projected precision of the Daya Bay experiment [34], LBNE10⁵, and full LBNE is about <4%, ~10%, and <5%, respectively. Therefore, by comparing the measured $\sin^2 2\theta_{13}$ value from the reactor experiments to that measured in accelerator experiments, one would rule out the specific hypothesis described above, given the unitarity is truly conserved.

The recent T2K ν_e appearance results [20] favors a larger value of $\sin^2 2\theta_{13}$ than that from the reactor $\bar{\nu}_e$ disappearance results. The statistical significance is at about 2σ level, whose actual value would depend on the assumption of the mass hierarchy and the value of CP phase δ . Such a difference at present is consistent with an explanation of a statistical fluctuation. If the difference persists with increased statistics, the hypothesis of existence of new physics would be favored. Otherwise, the phase space of new physics can be strongly constrained. Furthermore, as shown in Eq. (10), the existence of the fourth generation of sterile neutrino will likely not only change the effective mixing angle, but will also introduce additional spectrum distortion through non-zero δ_1 or δ_2 phases. Therefore, the wide band beam of LBNE together with its high statistics measurement of disappearance/appearance spectra would provide stringent tests for new physics.

There is actually another group of indirect unitarity tests. For example, one can see that Eq. (9) is the same one as $P(\nu_\mu \rightarrow \nu_e)$ at $L = 0$. Therefore, the search for appearance of ν_e with low backgrounds at very short baseline would effectively test unitarity. Such an experiment (e.g. ICARUS [42]) is indeed very powerful in constraining the phase space of sterile neutrino models, which are motivated by the LSND [43], MiniBooNe [44], and reactor [35] anomalies.

⁴ In our estimation, since both $U_{e 4}$ and $U_{\mu 4}$ are small, we have assumed that values of $|U_{e 3}|^2|U_{\mu 3}|^2$ and $4|U_{e 3}|^2 \cdot (|U_{e 1}|^2 + |U_{e 2}|^2)$ stay the same when we change from 3-neutrino model to 3-neutrino + 1-sterile neutrino model. This is not exactly true, as the components of the 3x3 PMNS matrix will change with non-zero $U_{e 4}$ and $U_{\mu 4}$. Additional small corrections should be applied. Nevertheless, these will not alter our conclusion.

⁵ LBNE10 represents the phase I of the LBNE program. LBNE10 contains a 10 kt liquid argon time projection chamber. The running time includes 5 years neutrino and 5 years antineutrino running with a 708 kW beam.

Conclusions: In this paper we illustrate the direct and indirect unitarity tests of the PMNS matrix with a few simple examples. In order to calculate the sensitivity of direct unitarity test of the first row $|U_{e1}|^2 + |U_{e2}|^2 + |U_{e3}|^2 \stackrel{?}{=} 1$, we approximate SNO results as a measurement of $|U_{e2}|^2 \cdot (|U_{e1}|^2 + |U_{e2}|^2) + |U_{e3}|^4$. A critical assessment of this formula can be found in Ref. [45]. We also neglect the matter effects in the long baseline ν_e appearance measurement in illustrating the power of indirect unitarity tests with θ_{13} .

Although direct unitarity tests appear to be extremely challenging given limited experimentally available oscillation channels, we show that the combination of the medium-baseline reactor experiment, short-baseline reactor experiments, and the SNO solar results will make it possible to perform the first direct and model independent unitarity test of the PMNS matrix. At 68% C.L., the combination of JUNO, Daya Bay, and SNO will test $|U_{e1}|^2 + |U_{e2}|^2 + |U_{e3}|^2 = 1$ at a 4% level. This level of accuracy can be substantially reduced with an improved constraint from solar neutrino measurements. In addition, by comparing the $\sin^2 2\theta_{13}$ values measured by the current generation reactor neutrino experiment vs. current/next generation accelerator neutrino experiments, one can perform an indirect unitarity test, which would put strong constraints on the possible new physics (e.g. sterile neutrino, non-standard interaction etc.) beyond the three-neutrino model. Such constraints will be further enhanced by the precision measurement of disappearance/appearance spectra with a wide band beam.

Acknowledgments: We would like to thank B. Viren and R. D. McKeown for fruitful discussions. This work was supported in part by the National Science Foundation, and the Department of Energy under contract DE-AC02-98CH10886.

* Corresponding author: xqian@bnl.gov

- [1] M. Goldhaber, L. Grodzins, and A. W. Sunyar. *Phys. Rev.*, **109**:1015, 1958.
- [2] J. Beringer *et al.* (Particle Data Group). *Phys. Rev.*, **D86**:010001, 2012.
- [3] R. D. McKeown and P. Vogel. *Phys. Rep.*, **394**:315, 2004.
- [4] B. Pontecorvo. *Sov. Phys. JETP*, **6**:429, 1957.
- [5] B. Pontecorvo. *Sov. Phys. JETP*, **26**:984, 1968.
- [6] Z. Maki, M. Nakagawa, and S. Sakata. *Prog. Theor. Phys.*, **28**:870, 1962.
- [7] K. Abe. *et al. Phys. Rev. Lett.*, **107**:241801, 2011.
- [8] M. H. Ahn *et al. Phys. Rev.*, **D74**:072003, 2006.
- [9] P. Adamson *et al. Phys. Rev. Lett.*, **110**:251801, 2013.
- [10] K. Abe *et al.* arXiv:1308.0465 (2013).
- [11] M. G. Aartsen *et al.*, arXiv:1305.3909 (2013).
- [12] S. Abe *et al. Phys. Rev. Lett.*, **100**:221803, 2008.
- [13] B. Aharmim *et al. Phys. Rev.*, **C72**:055502, 2005.
- [14] F. P. An *et al. Phys. Rev. Lett.*, **108**:171803, 2012.
- [15] F. P. An *et al. Chinese Phys.*, **C37**:011001, 2013.
- [16] Y. Abe *et al. Phys. Rev. Lett.*, **108**:131801, 2012.
- [17] J. K. Ahn *et al. Phys. Rev. Lett.*, **108**:191802, 2012.
- [18] P. Adamson *et al. Phys. Rev. Lett.*, **107**:181802, 2012.
- [19] K. Abe *et al. Phys. Rev.*, **D88**:032002, 2013.
- [20] M. Wilking (for T2K Collaboration), EPS (2013).
- [21] N. Agafonova *et al. Phys. Lett.*, **B691**:138, 2010.
- [22] K. Abe *et al. Phys. Rev. Lett.*, **110**:181802, 2013.
- [23] D. Ayres *et al.* [NOvA Collaboration] FERMILAB-DESIGN-2007-01 (2007).
- [24] C. Adams *et al.* arXiv:1307.7335 (2013).
- [25] X. Qian *et al.*, arXiv:1307.7406 (2013).
- [26] Y. F. Li *et al.* arXiv:1303.6733 (2013).
- [27] S. Kettell *et al.* arXiv:1307.7419 (2013).
- [28] K. Abe *et al.*, arXiv:1109.3262 (2011).
- [29] The PINGU collaboration, arXiv:1306.5846 (2013).
- [30] L. Wolfenstein. *Phys. Rev.*, **D17**:2369, 1978.
- [31] S. P. Mikheyev and A. Yu. Smirnov. *Sov. J. Nucl. Phys.*, **42**:913, 1986.
- [32] S. P. Mikheyev and A. Yu. Smirnov. *Sov. Phys. JETP*.
- [33] S. P. Mikheyev and A. Yu. Smirnov. *Nuovo Cim.*, **9C**:17, 1986.
- [34] X. Qian (on behalf of the Daya Bay Collaboration), arXiv:1211.0570 (2012).
- [35] G. Mention *et al. Phys. Rev.*, **D83**:073006, 2011.
- [36] C. Zhang, X. Qian, and P. Vogel. *Phys. Rev.*, **D87**:073018, 2013.
- [37] L. A. Mikaelyan and V. V. Sinev. *Phys. Atm. Nucl.*, **63**:1002, 2000.
- [38] P. Kyberd *et al.*, arXiv:1206.0294 (2012).
- [39] A. Porta *et al. IEEE Trans. on Nucl. Sci.*, **57**:2732, 2010.
- [40] K. M. Heeger, B. R. Littlejohn, and H. P. Mumm, arXiv:1307.2859 (2013).
- [41] M. Cribier *et al. Phys. Rev. Lett.*, **107**:201801, 2011.
- [42] D. A. Dwyer *et al. Phys. Rev.*, **D87**:093002, 2013.
- [43] G. Bellini *et al.*, arXiv:1304.7721 (2013).
- [44] J. D. Vergados, Y. Giomataris, and Yu. N. Novikov, arXiv:1105.3654 (2011).
- [45] V. N. Gavrin *et al.*, Proc. of Neutrino. Tele. 393 (2011).
- [46] J. M. Conrad *et al.*, arXiv:1307.5081 (2013).
- [47] M. Elnimr *et al.*, arXiv:1307.7097 (2013).
- [48] H. Chen *et al.*, FERMILAB-PROPOSAL-1030 (2013).
- [49] A. Gouvêa and T. Wytock. *Phys. Rev.*, **D79**:073005, 2009.
- [50] B. Bhattacharya, A. M. Thalapillil, and C. E. M. Wagner. *Phys. Rev.*, **D85**:073004, 2012.
- [51] M. Antonello *et al.*, arXiv:1307.4699 (2013).
- [52] A. Aguilar-Arevalo *et al. Phys. Rev.*, **D64**:112007, 2001.
- [53] A. A. Aguilar-Arevalo *et al.*, arXiv:1303.2588 (2013).
- [54] A. B. Balantekin. *J. of Phys. Conf. Ser.*, **337**:012049, 2012.